

PAPER • OPEN ACCESS

## Obtaining and characterization of nanostructured coatings of zirconia-alumina-ceria by thermal spray flame

To cite this article: L F Rodríguez *et al* 2019 *J. Phys.: Conf. Ser.* **1388** 012005

View the [article online](#) for updates and enhancements.

You may also like

- [Modified Cam-clay Model Parameters M of Kunming Red Clay](#)  
Xianru Liu, Jianguang Li, Ren Yi et al.
- [Application of red clay improved with sand at the foot of mountain in subgrade filling](#)  
Jianbao Fu and Li Zhang
- [Improvement technology research on red clay of Yuzhan expressway](#)  
Jiaying Zhang



**ECS**  
The  
Electrochemical  
Society  
Advancing solid state &  
electrochemical science & technology

**DISCOVER**  
how sustainability  
intersects with  
electrochemistry & solid  
state science research

# Obtaining and characterization of nanostructured coatings of zirconia-alumina-ceria by thermal spray flame

L F Rodríguez<sup>1</sup>, M Ferrer<sup>1</sup>, and G Peña<sup>1</sup>

<sup>1</sup> Grupo de Investigación en Instrumentación y Física de la Materia Condensada, Universidad Francisco de Paula Santander, San José de Cúcuta, Colombia

E-mail: luisfranciscorw@ufps.edu.co

**Abstract.** Zirconia, alumina and ceria powders were agglomerated, by granulator disk, to be used as raw material in the manufacture of coatings on red clay substrates by flame spray. Three mixtures of different compositions were made to determine which of them produces the most homogeneous and best bonded coatings. Likewise, the phase transformations that occur in the thermal spraying process were evaluated. The morphology and microstructure of the powders and coatings were determined by scanning electron microscopy and X-ray diffraction, respectively. Bimodal coatings were obtained, preserving the nanometric structure of the powders, homogeneous, low porosity and good adhesion.

## 1. Introduction

The thermal projection is a technique used worldwide in the making of coatings and the restoration of worn pieces. It has had a good reception in North America and Europe due to its vast amount of applications in the industry, thanks to the possibility of using it with any inorganic material.

There are different variations of the technique that depend mainly on the source of heat used to melt the raw material, the oldest is flame spray (FS), the flame is the result of the combustion of oxygen with a fuel, usually acetylene; it is versatile and cheap, commonly known as metallization, due to the ease of melting metals. Nowadays there have been efforts to understand the thermal conditions needed to make of that a particle, regardless the material melted with the flame [1]. Such studies have been successful and the researchers show coatings obtained with high fusion point ceramics like zirconia and alumina, with excellent physical, mechanic, thermal and anti-corrosive properties [2,3].

The success in the coatings begins with the quality of the raw material, it has to do with its chemical composition, size, and morphology, followed by the determination of the projection parameters to obtain the coatings, therefore, if the manufacturing of the raw material and the conditions to obtain the coatings are controlled, it is possible to build a coating with the necessary properties for a certain type of application [4].

The use of nanometric particles in thermal projection allows a partially nanostructured or bimodal coatings to be obtained, in which there are completely molten regions with non-molten nanometric particles, which improves the properties of the coatings.

In this study, the nanometric powders of zirconia, alumina and ceria were agglomerated by the granulator disk method to obtain micrometric agglomerates of nanometric particles [5]. Agglomerated particles of zirconia, alumina and ceria were used as raw materials for coatings made by FS, in red clay tiles to improve their mechanical properties.



## 2. Experimental

### 2.1. Nanometric powders agglomerates

The mixtures of powders were made using a commercial powder, Eutectic Castolin® MetaCeran reference of 25088 of  $ZrO_2$  – 36% weigh of  $Al_2O_3$ , with a size distribution of  $d_{10} = 15 \mu m$  y  $d_{90} = 95 \mu m$  and nanometric powders of  $CeO_2$  100% pure, with an approximate size of  $1.5 \mu m$ .

With the aim to homogenize the compounds and the size of the powders, they were grinded in a planetarium mill during 20 minutes to 300 rpm, and then they were agglomerated using a pelletizer disk designed and built by the group GIMACYR of the “Universidad de Antioquia” [5]. The equipment consists of an engine attached to a structure with a variable slant of  $15 - 90^\circ$ , which transmit a rotational movement to a stainless-steel disk of 30 cm in diameter. The parameters used are summarized in Table 1. [5,6]. Three mixtures were made, with different weight concentrations of zirconia, alumina and ceria, named as P1, P2 and P3.

**Table 1.** Used parameters in the agglomeration.

Gathering parameters of the nanometric powders	Values
Binding flow ml/min	2
Binding jet (pressure)(MPa)	0.05
Disk slant angle	$80^\circ$
Disk rotation speed (rpm)	76–80
Nanometric powder mass (g)	15–17
Binding volume (ml)	5.5
Agglomeration time (s)	180

### 2.2. Powders and coatings characterization methods

**Structure and morphology:** The elemental chemical composition was determined by energy dispersive X-ray spectrometer (EDS), the microstructure was made through Rietveld refinement using X'pert HighScore Plus software, which compares the X rays diffraction pattern lines with the data base patterns PDF-2 of the International Center for Diffraction. The diffractograms were obtained with a powder diffractometer BURKER brand, D8 ADVANCE model with Da Vinci geometry, under these conditions: voltage (40 KV), current 40 (mA) divergence slot 0,6 (mm) main soller slot  $2.5^\circ$ , sampling 0,002035  $2\theta$ , measuring range  $3.5 - 70^\circ 2\theta$ , radiation Cu –  $K_{\alpha 1}$  nickel filter, LynxEye lineal detector, type of scan stepped, sampling time 0,6 seconds [7,8].

For morphology analysis, samples were prepared metallographically, according to ASTM E 1920-03 [8], these were mounted in low shrinkage polymer resin and allowed to dry for 48 hours, then cut with a diamond disk at high speed, in such a way as to expose the cross-section of the coating. Then, a roughing with SiC sand paper of different grains was carried out with a sequence of P1000, P1200, P1500, P2000 and P2500, finally, it was proceeded with a polishing with a  $1 \mu m$  diamond paste.

Porosity in coatings was determined via image-analysis technique using optical microscopy (OM). At least 30 optical microscopy images were taken for each coating, as specified in the standard rule ASTM 2109 [9], for this type of coatings, analyzed with the free ImageJ software [10].

**2.2.1. Adhesion.** The adhesion of the coatings to the substrate was determined with the technique known as "Pull Off", with which the highest perpendicular (direct) tension that the coating could withstand is determined, before separating from the substrate. The failure happens along the weakest plane within the system consisting of the test equipment, the adhesive material, the coating and the substrate; the surface of the fracture is exposed. In general, stress from tension or direct adhesion can be obtained as the ratio between the maximum forces obtained in the test and the area of the interface; theoretically, this formulation will be valid, provided that the failure occurs completely in this area [11].

### 3. Results and discussions

#### 3.1. Chemical composition of the mixtures

The composition of each one of the mixtures for the production of the agglomerates is shown in the Table 2, where the quantity of oxide of cerium increases, whereas the zirconia and the alumina decrease. The compounds were called P1, P2 and P3, where the number increases as the amount of ceria does the same.

**Table 2.** Chemical composition in weight volume of the mixture obtained, P1, P2 and P3.

Powder	Volume %			Weight %		
	ZrO <sub>2</sub>	Al <sub>2</sub> O <sub>3</sub>	CeO <sub>2</sub>	ZrO <sub>2</sub>	Al <sub>2</sub> O <sub>3</sub>	CeO <sub>2</sub>
P1	48.83	41.03	10.14	53.8	30.9	15
P2	46.85	39.37	13.78	50.6	29.1	20
P3	44.79	37.64	17.57	47.5	27.3	25

#### 3.2. Characterization of agglomerated powders

The powder size distribution is shown in Table 3. The minor size was obtained for the powders P1 and P3 where  $d_{50}$  was 5.5 and 9.9  $\mu\text{m}$  micrometers respectively, showing a great quantity of very small agglomerates due to the fact that the quantity of binder was not enough to compact the particles and to provide a major union force to them, whereas for the powder P2  $d_{50}$  it was of 58  $\mu\text{m}$  micrometers, managing to have agglomerates of great size up to 82 micrometers which shows that the conditions of agglomeration are efficient for this composition [12]. The morphology is shown in Figure 1, P2 is the powder that presents a better agglomeration, irregularly, and different gray scales are observed, where the darkest areas correspond to alumina, the lightest to ceria and the intermediate ones to zirconia.

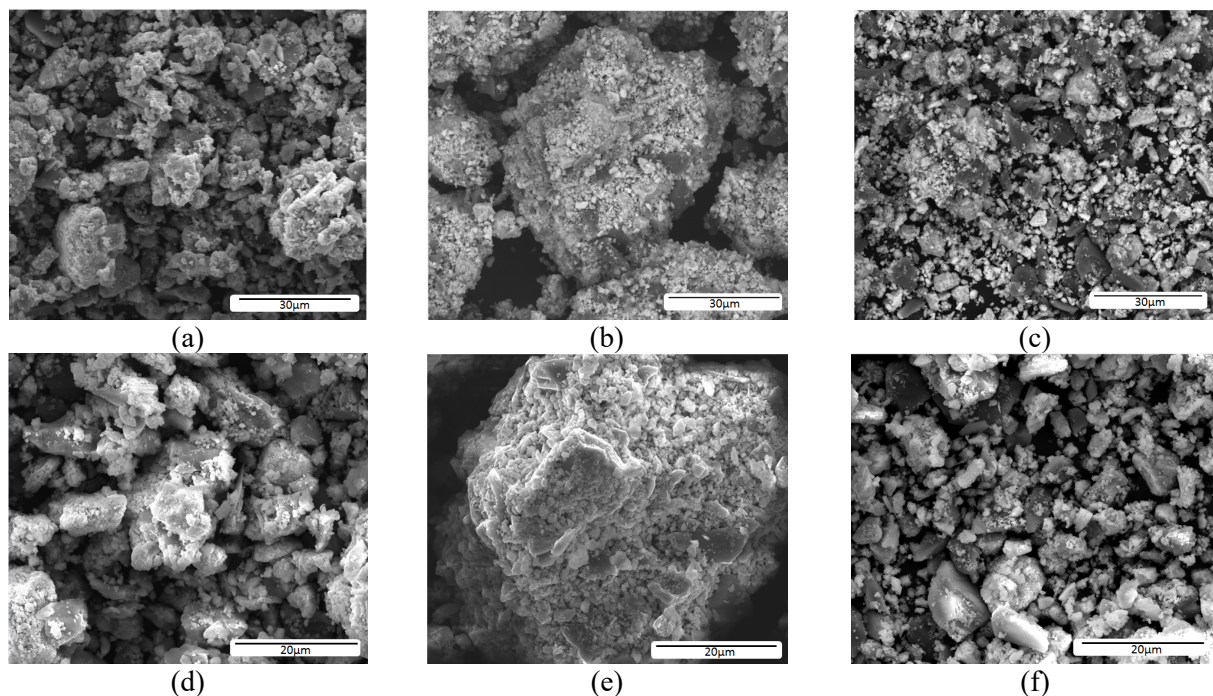


**Figure 1.** SEM micrographs showing the (a) P1 powder and (d) an increase to P1. (b) P2 powder and (e) an increase to P2 and (c) P2 powder and (f) an increase to P2.

The Rietveld refinement showed that the percentage of the phases present matches the initial composition of the powders, see Table 4.

**Table 3.** Size distribution of agglomerated powders.

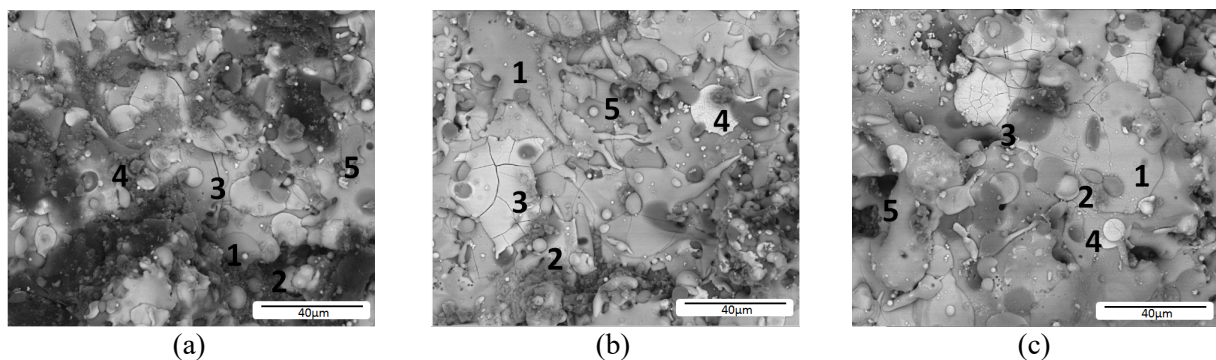
Size distribution ( $\mu\text{m}$ )	P1	P2	P3
$d_{10}$	--	35	2.5
$d_{50}$	5.5	58	9
$d_{90}$	23	82	20
$d_{\text{prom}}$	$9.71 \pm 8.42$	$61.73 \pm 8.42$	$6.73 \pm 4.27$

**Table 4.** Percentage of phases found in powders P1, P2 y P3.

	ZrO <sub>2</sub>	Al <sub>2</sub> O <sub>3</sub>	CeO <sub>2</sub>	Adjustment quality (GoF)
P1	63.1%	26.6 %	10.3%	2.83641
P2	57.2%	28.1%	14.7%	2.87158
P3	42.6%	41.1%	16.3%	2.26456

### 3.3. Morphology of coatings

The superficial morphology of the coatings: The coatings are named C1, C2 and C3, obtained with powders P1, P2 and P3 respectively. In Figure 2, the characteristics of the coatings are shown as: 1. Splats, 2. Unfused or semi-fused particles, 3. Cracks in the splats, 4. bimodal structures and 5. Pores, among others [13]. The coatings were formed by splats of well molten particles. In the coating C1 and C3, the splats have the form of a disc (pancake), which is beneficial since it allows to obtain uniform coatings and with low porosity, nevertheless, the covering C2, shows a few splats with splash which allow us to say that the particles were well molten and with a lot of thermocinetic energy. In all the cases cracks were visible in the splats which can happen due to the thermal shock and the difference in the coefficients of thermal expansion of the compounds, in addition bimodal zones formed by nanometrics wrapped particles by micrometric well molten particles can be seen, preserving his nanometric structure, which is beneficial since it improves its behavior against fracture tenacity and properties like the conductivity and the thermal diffusion [14].

**Figure 2.** Surface morphology of coatings (a) C1, (b) C2 and (c) C3.

Transverse morphology of the coatings: The Figure 3 shows the morphology of the coatings transversally. It can be appreciate that they are uniform, formed for lamellas of different color in the scale of gray, where the darkest correspond to the alumina, the clearest and brilliant to the oxide of cerium and the intermediate ones to the zirconia, such as the reported for A. Gonzalez et al [2]. Stacking failures can also be found, which occur due to irregularities of the substrate or the previously deposited coating layers. Circular pores correspond to bubbles caused by the evaporation of the particles [15]. One of the characteristics of these coatings are the bimodal zones, formed by non-molten nanometric particles and completely molten particles. This characteristic gives an extra value to the coating, since these areas dissipate the propagation energy of a crack, thus increasing the fracture toughness. In Figure 3, the characteristics described above are named as: 1. Lamella, 2. Unfused particles, 3. Interlamellar cracks, 4. Vertical cracks, 5. Bimodal areas, 6. Pores and 7. Substrate.

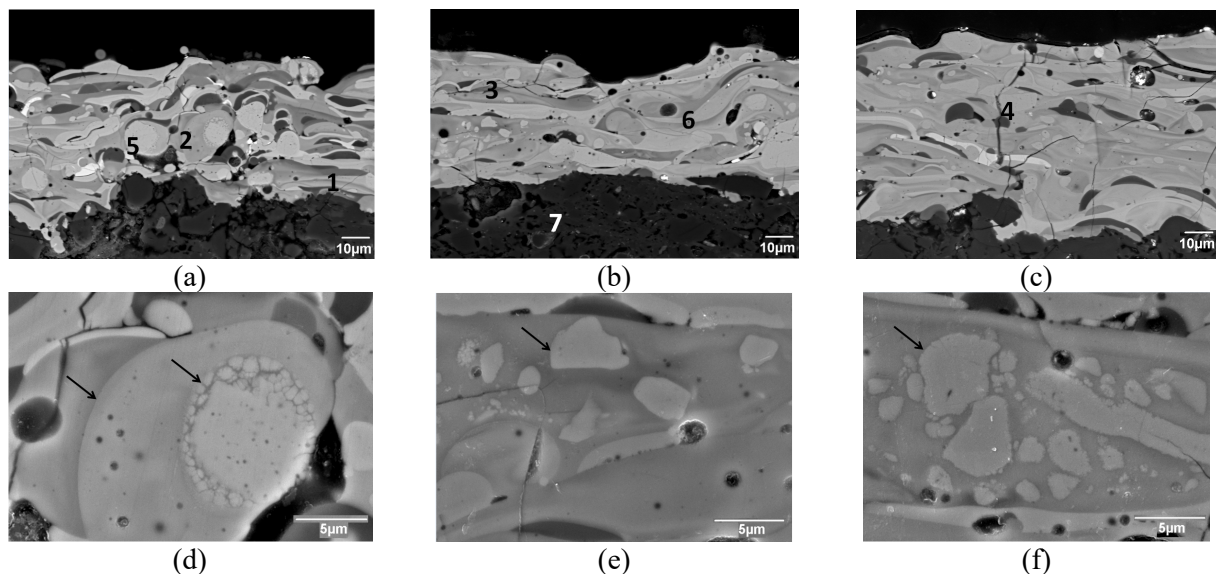


**Figure 3.** SEM micrographs show the cross section of (a) C1, (b) C2 and (c) C3. The micrographs shown in (d), (e) and (f) correspond to an approach to their morphology.

### 3.4. Structure of the coating

The coatings made by thermal projection are accompanied by phase transformations during their process due to heating and rapid solidification and cooling during the production process, which causes the presence of crystalline and amorphous phases, therefore, the phases in the coatings they are different from the phases present in the raw materials. In the Figure 4, the phases for each of the coating with different crystalline structures can be seen, it can be observed that crystallinity decreases with the increase in ceria weight percentage. Two amorphous zones in  $2\theta = 30^\circ$  and  $50^\circ$  can be seen. It is observed in a high percentage of the zirconia retained in its tetragonal phase, this is due to the presence of cerium oxide, in addition a cubic phase of cerium oxide and zirconia appears that contributes to the toughness of the coating. Two phases demonstrate alumina; an alpha phase, which corresponds to the one that did not merge when passing through the flame and the hardness of the cover and another, a gamma phase that reached a temperature higher than  $1000^\circ\text{C}$  until the fusion (see Table 5) [15,16].

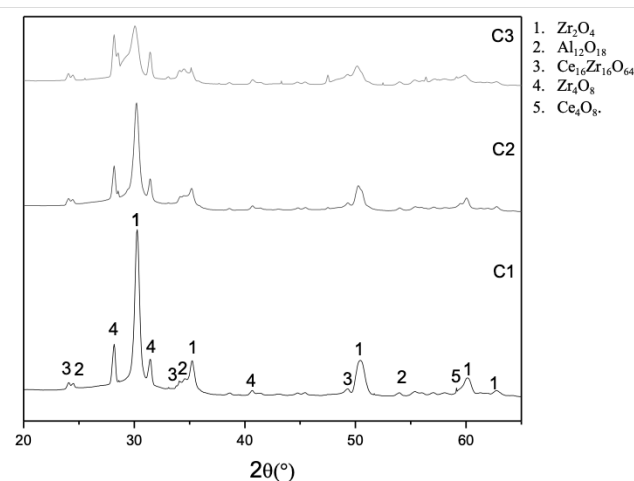


**Figure 4.** XRD patterns of spectra for coatings C1, C2 and C3.

**Table 5.** Percentage of phases presents in the coatings C1, C2 and C3

Coating	t-Zr <sub>2</sub> O <sub>4</sub>	c-CeO <sub>2</sub>	m-Zr <sub>2</sub> O <sub>4</sub>	$\alpha$ -Al <sub>2</sub> O <sub>3</sub>	m-Al <sub>2</sub> O <sub>3</sub>	c-CeZrO <sub>4</sub>	Adjustment quality (GoF)
C1	86.4%	0.2%	12.8%	0.3%	0.3%	0.1%	2.52825
C2	82.3%	0.4%	15.9%	0.1%	0.1%	1.2%	1.71665
C3	60.7%	2.5%	20.8%	1.9%	0.1%	14%	1.59927

### 3.5. Thickness, porosity and adhesion of coatings

According to the results showed in the Table 6, the thickness does not show a direct relation with the size of the powders, on the contrary, the powder P2 of major size, it generated the thinnest coating, it is important to indicate that in the three cases the thickness is thin, in comparison to the results obtained by A. Gonzalez [3], who made coatings with these materials, under the same technology and with similar conditions, the difference is that in the size of the powder used. The porosity found is lower than that reported by A. González [16]. When alumina and zirconia are mixed with cerium oxide, the melting point decreases, which allows very molten particles, small particles <5  $\mu\text{m}$ , melt easily and are stacked filling the imperfections left by semi-molten particles.

With respect to adhesion, the C2 coating has a slightly higher value; however, all samples have a very similar value. The most common fault in the samples is the cohesive type that gives off part of the ceramic base, which shows an excellent adhesion of the coatings on the substrate.

**Table 6.** Physical properties of coatings C1, C2 and C3.

Coating	Thickness ( $\mu\text{m}$ )	Adhesion Lb.in <sup>-2</sup> (Psi)	Porosity %
C1	47.39 $\pm$ 4.92	1060	1.516 $\pm$ 0.533
C2	42.77 $\pm$ 12.82	1130	1.028 $\pm$ 0.499
C3	56.33 $\pm$ 9.46	1060	1.147 $\pm$ 0.567

## 4. Conclusions

The characteristics of the coatings obtained by FS depend largely on the properties of the powders used, mainly on their composition and size. The method of granulator disk is useful for agglomerating zirconium-alumina-ceria powders, obtaining micrometric powders of adequate size and mechanical strength sufficient to be manipulated without fracturing in the thermal projection process.

The coatings obtained showed to be uniform of low porosity, with a good adhesion and with bimodal structures, preserving the nanometric structure of the powders, which improves the properties of the coatings.

## Acknowledgement

The researchers of this work thank the research group GIMACYR of the Universidad de Antioquia de Colombia, for their participation in the preparation and characterization of the coatings.

## References

- [1] Cadavid Iglesias E, Parra Velásquez C and Vargas Galvis F 2016 Estudio de llamas oxiacetilénicas usadas en la proyección térmica *Revista Colombiana de Materiales* **9** 15-26
- [2] Ferrer Pacheco M Y, Moreno Téllez C M and Vargas Galvis F 2018 *Recubrimientos de circonia y alúmina por proyección térmica con llama: parámetros para obtener recubrimientos de alto punto de fusión* (Tunja: Universidad Pedagógica y Tecnológica de Colombia)
- [3] González Hernández A G 2014 *Estudio del comportamiento a alta temperatura de recubrimientos nanoestructurados elaborados por proyección térmica por combustión y plasma a partir de polvos y suspensiones* (Francia: Université de Limoges)
- [4] Morales Torres J A, Olaya Flórez J J and Rojas Molano H F 2012 Una aproximación a la tecnología de proyección térmica *AVANCES Investigación en Ingeniería* **9(2)** 60-71

- [5] Arias Gómez J A, Vargas Galvis F and López M E 2014 Aglomeración de partículas nanométricas de  $ZrO_2$  mediante peletización en tambor para uso en proyección térmica por llama oxiacetilénica *Revista Colombiana de Materiales* **5** 290-295
- [6] Gil López J F, Rodríguez J E, Vargas F, López E and Restrepo E 2014 Mejoramiento de la estructura de los recubrimientos de  $Al_2O_3$ -43% elaborados mediante la técnica de proyección térmica por llama oxiacetilénica a partir de los parámetros de proyección *Revista Colombiana de Materiales* **5** 120-126
- [7] Valle J, Anglada M, Ferrari B and Baudín C 2015 Processing, nanoindentation and scratch testing of alumina-coated YTZP *Boletín de la Sociedad Española de Cerámica y Vidrio* **54(4)** 133-141
- [8] American Society for Testing and Materials (ASTM) 2014 *Standard guide for metallographic preparation of thermal sprayed coatings, ASTM E1920-0320* (USA: American Society for Testing and Materials)
- [9] American Society for Testing and Materials (ASTM) 2014 *Standard test methods for determining area percentage porosity in thermal sprayed coatings, ASTM E2109-01* (USA: American Society for Testing and Materials)
- [11] American Society for Testing and Materials (ASTM) 2014 *Standard guide for pull-off test for FRP-concrete interfaces, ASTM D7522* (USA: American Society for Testing and Materials)
- [12] Vargas F 2010 *Élaboration de couches céramiques épaisses à structures micrométriques et nanométriques par projections thermiques pour des applications tribologiques* (Francia: Université de Limoges)
- [13] Pawlowski L 2008 *The science and engineering of thermal spray coatings* (Washington: John Wiley & Sons)
- [14] González A G, Ageorges H, Rojas O, López E, Hurtado F M and Vargas F 2015 Efecto de la microestructura y de la microdureza sobre la resistencia al desgaste de recubrimientos elaborados por proyección térmica por plasma atmosférico a partir de circon-a-alúmina, circon-a-itra y circon-a-ceria *Boletín de la Sociedad Española de Cerámica y Vidrio* **54(3)** 124-132
- [15] González A, López E, Tamayo A, Restrepo E and Hernández F 2009 Análisis de la microestructura y de las fases de elaborados por proyección térmica *DYNA* **77(162)** 151-160
- [16] González A, Henao J, Díaz A F, López E and Vargas F 2013 Influencia de los parámetros de proyección térmica en la microestructura de los recubrimientos de circon-a-alúmina y circon-a-ceria usados como barreras térmicas *Revista Latinoamericana de Metalurgia y Materiales* **33(2)** 272-281